Peptidomimetic-based approach toward inhibitors of microbial trimethylamine lyases

Gabr, M. T., Deganutti, G. & Reynolds, C. A.

Original citation & hyperlink:
Gabr, MT, Deganutti, G & Reynolds, CA 2021, 'Peptidomimetic-based approach toward inhibitors of microbial trimethylamine lyases', Chemical Biology and Drug Design, vol. 97, no. 2, pp. 231-236.
https://dx.doi.org/10.1111/cbdd.13775

DOI 10.1111/cbdd.13775
ISSN 1747-0277
ESSN 1747-0285

Publisher: Wiley

Multi-objective optimization of conventional and non-conventional material removal processes using a visual contrast-based fruit fly algorithm

Abstract

Using optimal parameters for machining operations is essential so as to achieve high product quality, maximize profit; increase productivity and save resources for sustainability. In this work a fruit fly algorithm based also on visual contrast is applied to solve a number of significant machining processes to manufacturing industry; most of the non-conventional, namely turning; focused ion beam micro milling; laser cutting; wire electro-discharge machining and micro wire-electro discharge machining. Optimization process for these manufacturing processes is achieved through the application of robust regression equations considered as objective functions towards the goal of providing qualitative non-dominated optimal solutions in the form of Pareto fronts for each of the machining processes mentioned. The results obtained using the proposed fruit fly intelligent algorithm are compared to those obtained by two special heuristics; the multi-objective grey-wolf optimization algorithm (MOGWO) and the multi-objective multi-universe optimization algorithm (MOMVO) for the same problems. The results are also compared to those available in the literature referring to the aforementioned machining operations and the usage of other intelligent variants of evolutionary algorithms.

Keywords: Machining operations; multi-objective optimization; visual contrast; contrast-based fruit fly algorithm; intelligent algorithms

1. Introduction

Manufacturing has been integrated with modern methods in design, analysis and non-conventional production equipment in order to contribute to economy and consumers' prosperity. Engineering analysis tools are currently implemented to design modern and versatile products, test functionality and generate consistent plans for numerical control part programming. Aiming towards satisfying production requirements in terms of quality and efficiency, stringent procedures as well as public awareness impose an additional concern to manufacturing industry; that of environmental protection. In order to fulfill the aforementioned goals and meet the demands, both hardware and software should be used such that the best possible performance is reached.

The performance of any manufacturing process is significantly affected by its corresponding process parameters' settings, hence; optimizing them plays key role for the successful production. To

optimize the selection of values for process parameters the comprehensive knowledge of the systems involved and the establishment of realistic objectives are needed. When it comes to the broader field of manufacturing as well as other branches of engineering, optimization problems suggest multiple combinations of parameter values that may converge to optimal solutions. This has drawn the researchers' interest towards the development and the application of heuristic-based modules such as evolutionary algorithms and swarm intelligence to optimize parameter settings for machining processes.

Even though conventional manufacturing processes are still useful in production, non-conventional operations are now deployed to increase quality. A very popular material removal process is conventional turning where material is removed by rotating the cylindrical part and cutting it using a typical single-edge high speed steel tool or an insert attached to a tool holder. Turning is a very productive machining process for which numerous studies have been conducted either to examine the significance of effects of individual process parameters on performance criteria or to optimize machinability characteristics, i.e. surface roughness, material removal rate, cutting force, etc., by means of soft computing and/or artificial intelligence techniques. Palanikumar et al. (2009) conducted experiments using a conventional lathe and cylindrical glass-fiber reinforced plastic (GFRP) work pieces so as to study the effect of machining parameters cutting speed, feed rate and depth of cut and find the optimal combination to satisfy conditions for high material removal rate; minimum tool flank wear and minimum surface roughness. Based on the results obtained a statistical analysis was then conducted to produce second-order polynomial prediction models and consider them as objective functions for an intelligent algorithm. These models were evaluated by the non-dominated sorting genetic algorithm (NSGA-II) proposed by Srinivas and Deb (1995). The necessity to produce modern small-scale/micro-scale products has led to the implementation of fast and accurate methods such as the focused ion-beam micro-milling (FIB). FIB micro-milling has an important application to semi-conductors; optical lithography masks; magnetic parts, etc., whilst it can handle any kind of material such as metallic, non-metallic, ceramic, biomaterials, etc. For this particular non-conventional micro-milling process, Bhavsar et al. (2012) adopted an L16 orthogonal array to design and conduct experiments using a FIB machine and cemented carbide as the work material under the scope of maximizing material removal rate and minimizing surface roughness. The effects of influential parameters related to this machining process were studied and analyzed to create empirical models to predict the aforementioned responses. Bhavsar et al. (2015) continued their previous work to optimize material removal rate and surface roughness using a genetic algorithm (GA). Pandey and Dubey (2012) employed an L27 Taguchi orthogonal array to design and conduct laser cutting experiments using Ti6Al4V sheets of 1.4mm thickness for studying the optimal conditions to minimize surface roughness and kerf taper. By developing second-order regression models a GA was then implemented to optimize the process. Garg et al. (2012) presented results concerning the optimization of the wire electro-discharge machining (wEDM) process. Their experiments were established by adopting the Box-Behnken design which is a variant of response surface methodology. In their experiments a CNC wire-cut machine was used and equipped with brass wire of 0.25 mm thickness. Ti 6-2-4-2 rectangular plates (200mm x 200mm x 20.4mm) were used as working materials. The purpose of their study was to find combinations among process parameters capable of simultaneously maximizing cutting speed and minimizing surface roughness. NSGA-II algorithm was applied to regression models corresponding to experimental results to evaluate them as objective functions. Kuriachen et al. (2015) moved towards a similar fashion to first study and then optimize the process parameters corresponded to micro-wire electro-discharge machining (mwEDM) with Ti6Al4V as a work material. Their experiments were designed using an L9

orthogonal array whereas second-order regression models were developed to predict the responses. In their work a fuzzy logic model was also developed to simulate the non-linear behavior of the problem at hand. The model was developed by adopting Sugeno-type fuzzy rules and average strategy as the defuzzification method. The particle swarm optimization algorithm (PSO) was finally implemented to maximize material removal rate and minimize surface roughness.

This work aims at exploring the possibility of improving further the results from the optimization efforts related to conventional and non-conventional machining processes such as those presented in the literature section above. To accomplish this aim a new fruit fly optimization algorithm based also on the visual contrast (c-mFOA) has been developed and is proposed to solve the optimization problems of the machining processes selected namely, turning; focused ion-beam micro milling; laser cutting; wire electro-discharge machining and micro-wire electro-discharge machining. Along with the c-mFOA proposed in this work, two other variants of intelligent algorithms were added to the research namely multi-objective grey wolf optimizer - MOGWO (Mirjalili et al. 2016) and multi-objective multi-universe optimizer – MOMVO (Mirjalili et al. 2017). Results deal with the qualitative and practical examination of Pareto-fronts corresponding to each of the considered machining processes and the non-dominated solutions obtained by implementing c-mFOA are compared to those reported by previous researchers who have implemented other intelligent algorithms like NSGA-II (Srinivas and Deb 1995), GA, PSO, MOTLBO (Zou et al. 2014) and NSTLBO (Rao et al. 2016). To substantiate the practical meaning of the results obtained in the cases where small differences in magnitudes were experienced, two-sample t-tests were conducted to examine whether the results' differences were statistically significant or not. For rigorous and fair comparisons among results the number of generations as well as other crucial settings for algorithm-specific parameters was adjusted according to indications from previous research efforts reported for the same problems.

2. Contrast-based fruit fly optimization algorithm

Fruit fly optimization algorithm mimics the behavior of fruit flies to detect odours by using their keen sense of smell. Their osphresis allows them to track sources of food up to 40 km away with regard to their current position. Moreover fruit flies can follow the direction of their fellows owing to their excellent vision. The first fruit fly algorithm was proposed by Pan (2012) to solve a financial distress problem.

To simplify the presentation of fruit fly algorithm a one-dimensional problem is considered. As a first step the algorithm determines a fruit fly in a random position; let it be $x_o = [X_{01}, Y_{01}]$. Thereby a swarm of fruit flies x_i is randomly generated. The swarm's magnitude is *N-1* whilst $x_i = [X_{i1}, Y_{i1}] = [X_{01}+rand, Y_{01}+rand]$ with *rand* to represent a random number in the range [0, 1]; rand $\in$ [0, 1]. For each x_i fruit fly in (*N-1*) swarm the distance $D_{i1} = \sqrt{X_{i1}^2 + Y_{i1}^2}$ from the coordinate system's origin is computed to be further taken as an input for determining the objective function's value, $S_{mi} = f(D_{i1})$. The fruit fly with the best objective function value is identified and the rest of the flies are randomly relocated around it. The algorithm operates until a maximum number of generations is reached.

As it occurs to genetic – evolutionary algorithms (GAs-EAs), exploitation and exploration capabilities are mandatory for swarm intelligence systems as well. Li et al. (2014) presented the first fruit fly algorithm with modified (enhanced) features in terms of exploitation and exploration. In their algorithm the fruit fly with the worst performance is substituted by the one achieves the best. Compared to the

original fruit fly algorithm of Pan (2012), only a single fruit fly is replaced instead of the entire swarm. In addition the fruit flies are randomly located around the vicinity of fruit flies that exhibited advantageous performance rather than that of a single best fruit fly. Pan (2013) presented another modification on the original fruit fly's algorithm architecture. The modification deals with the representation of the input parameter D_{i1} which was modified as $\frac{D_{i1}}{1+D_{i1}^2\times(0.5-\delta)}$ where δ is a problem-dependent, algorithm-specific parameter. Another improvement of the explorative rate of the fruit fly algorithm has been discussed in the work of Pan et al. (2014). Their work suggests the adaptive food search radius instead of determining constant values for it. The expression for this adaptive food search mechanism id given in Eq. 1, where λ_{min}, λ_{max} are the minimum and maximum search radii; *iter* is the iteration number and $iter_{max}$ is the maximum number of iterations.

$$\lambda = \lambda_{\max} \times \exp\left(\ln\left(\frac{\lambda_{\min}}{\lambda_{\max}} \right) \times \frac{iter}{iter_{\max}} \right) \tag{1}$$

Fruit flies are computed as $x_i = [X_{01}+\lambda \times rand, Y_{01}+\lambda \times rand]$. In the work of Yuan et al. (2014) a multi-swarm fruit fly algorithm is proposed to improve exploration of the original fruit fly algorithm. According to this scheme the initial fruit fly swarm is divided to several sub-swarms; usually 4 to 10 so as to independently explore the solution space and converge to global optimum. Wu et al. (2015) suggested another alternative to enhance the fruit fly algorithm's exploration. In their work a normal cloud generator is used and is dependent of three algorithm-specific parameters, namely; average value E_x; entropy E_n and hyper-entropy H_e. The average value corresponds to the possibility of finding food solutions; entropy reflects the search domain and hyper-entropy indicates the stability of the search. That is, the discrete degree increases with the increase of hyper-entropy. Entropy is continuously decreasing according to the relation given in Eq. 2 where E_{n_max} and α, are user-defined algorithm parameters. Hyper entropy H_e has a constant relation to Entropy E_n; $H_e = 0.1 \times E_n$.

$$En = En_{\max} \times \left(1 - \frac{iter}{iter_{\max}} \right)^{a} \tag{2}$$

Another noticeable enhancement of the original fruit fly algorithm was achieved by Mitic et al. (2015) based on the Chaos theory. What is suggested n their work, is the relocation of fruit flies using the expression given in Eq. 3 where x_i [k+1] and x_i [k] are the new and old positions respectively, whilst *alpha* is a chaotic variable. The authors investigated the influence of ten different maps – including Chebyshev, Circle, Gauss/Mouse, Logistic and Tent – used for describing the chaotic behavior.

$$x_i[k+1] = x_i[k] + alpha \times \left(x_i[k] - x_0[k] \right) \tag{3}$$

2.1. Proposed Contrast-based fruit fly optimization algorithm (c-mFOA)

Recent biological studies have shown that fruit flies exhibit a more complex food search mechanism than the one initially realized and modeled by Pan (2012). If fruit flies fail to find food using osphresis they start their exploration via their visual contrast. A good example of their behavior in terms of their visual contrast as an explorative asset is that of having a glass of wine where the glass would play the role of the contrasting shape and the wine would be the source under interest. Fruit flies approach the source and if there is not something to eat they continue to forage. In addition it has been found that fruit flies surge when the scent is strong and cast when it becomes weaker. Last but not least, it was observed that fruit flies present a response delay. It is believed that fruit flies developed these features to compensate for the chaotic movement of odours, particularly outdoors in the wind.

The aforementioned natural mechanisms of fruit flies have been fully realized in this work and for the first time in the literature the proposed algorithm is implemented to solve different multi-objective optimization problems related to manufacturing technology. So far the fruit fly algorithm proposed in this paper has been used for optimizing the large number of members comprising trusses in the field of structural engineering (Kanarachos et al. 2017). To facilitate the description of the proposed fruit fly algorithm (c-mFOA) a one-dimensional problem is discussed. Assume a coordinate system and a position of a fruit fly with the coordinate $x_o = [X_{01}, Y_{01}]$. The swarm of the rest *N* fruit flies is randomly scattered in the vicinity of x_o according to Eq. 4.

$$\begin{aligned} X_{i1}[k] &= X_{01}[k]\times\left(1+M\times\left(2\times rand_{N_{res}}-1\right)\right), i=1,\ldots,N \\ Y_{i1}[k] &= Y_{01}[k]\times\left(1+M\times\left(2\times rand_{N_{res}}-1\right)\right), i=1,\ldots,N \end{aligned} \tag{4}$$

In Eq. 4 *k=1,2,…,K* is the iteration number, *N* is the size of the swarm and $rand_{N_{res}}$ is a random number from a uniform discrete distribution defined in the interval $[1,N_{res}]$. The use of a discrete distribution is not observed in nature, but it constitutes a feature introduced to the algorithm for its improved performance in multi-parameter engineering optimization problems. *M* is a scaling parameter determining how coarse or fine the search strategy is.

Each fruit fly $x_i[k] = [X_{i1}[k], Y_{i1}[k]]$ is assigned a value based on the Euclidean distance between the fruit fly and the coordinate system's origin; $DI_{i1}[k]$ (Eq. 5 and 6).

$$DI_{i1}[k] = \sqrt{\left(X_{i1}[k]\right)^2+\left(Y_{i1}[k]\right)^2} \tag{5}$$

$$DI_{i1}[k] = \frac{1}{DI_{i1}[k]} \tag{6}$$

$DI_{i1}[k]$ is sensitive for fruit flies located in the vicinity of the coordinate system's origin, as opposed to those positioned far from it. This implies that a good search strategy should start close to the origin. Each fruit fly is assigned a ''smell concentration'' $Sm_i[k]$ at $x_i[k]$ determined by the objective function value $Sm_i[k] = f\left(x_i[k]\right) = fx_i\left(DI_{i1}[k]\right)$. A small objective function value corresponds to a position

with high smell concentration. The fruit flies are ranked, on the basis of their smell concentration, and the fruit fly x*[k] that achieves the highest smell concentration Sm*[k] (lowest value for the objective function) at position [X*[k], Y*[k]] is identified. That is, if the smell concentration Sm*[k] is better than that of the current point of attraction Sm_0 [k]. Thus, if $Sm^*[k] < Sm_0$ then $X_0[k+1] = X^*[k]$ and $Y_0[k+1] = Y^*[k]$ whilst x*[k] becomes the new attraction point. The algorithm is terminated when the maximum number of *K* iterations has been reached.

When the stimulus changes fruit flies do not respond immediately: a delay occurs before changing the food search strategy. Delay is constant and independent of other algorithm-specific parameters. This behavior is idealized and modeled in the c-mFOA algorithm. In case the objective function improves over the last *κ* iterations, *κ* represents the response delay, the swarm enters the ‘‘surging” phase, during which the flies move towards the attraction point x_0[k] at a greater speed. Thus; if $\left(Sm_0[k] < Sm_0[k-\kappa]\right)$ then $M[k+1] = c \times M[k]$. In case the objective function does not change over the last *κ* iterations then the swarm enters the ‘‘visual contrast” attraction phase, in which flies are attracted by the point $x^{\cdot\cdot}[k]$ that achieves the lowest smell concentration $Sm^{\cdot\cdot}[k] = \max\left(Sm_i[k]\right)$. If $\left(Sm_0[k] = Sm_0[k-\kappa]\right)$ then $X_0[k+1] = X^{\cdot\cdot}[k]$ and $Y_0[k+1] = Y^{\cdot\cdot}[k]$ where *k* is the current iteration. In case the objective function worsens over the last *κ* iterations, the swarm enters the ‘‘casting” phase, in which flies return to the previous current best $x_0[k-\kappa]$ and continue the search at a constant speed. Thus; if $\left(Sm^*[k] > Sm_0[k-\kappa]\right)$ then $X_0[k+1] = X_0[k-\kappa]$ and $Y_0[k+1] = Y_0[k-\kappa]$. The last step is based on the ability of fruit flies to remember and choose on the basis of how well or bad a memory was. In c-mFOA the constraints are dealt using the penalty function approach. The constrained optimization problem is formulated as an unconstrained one by augmenting the response function *R(x)* (Kanarachos et al. 2017). The c-mFOA’s operational workflow is depicted in Fig.1.

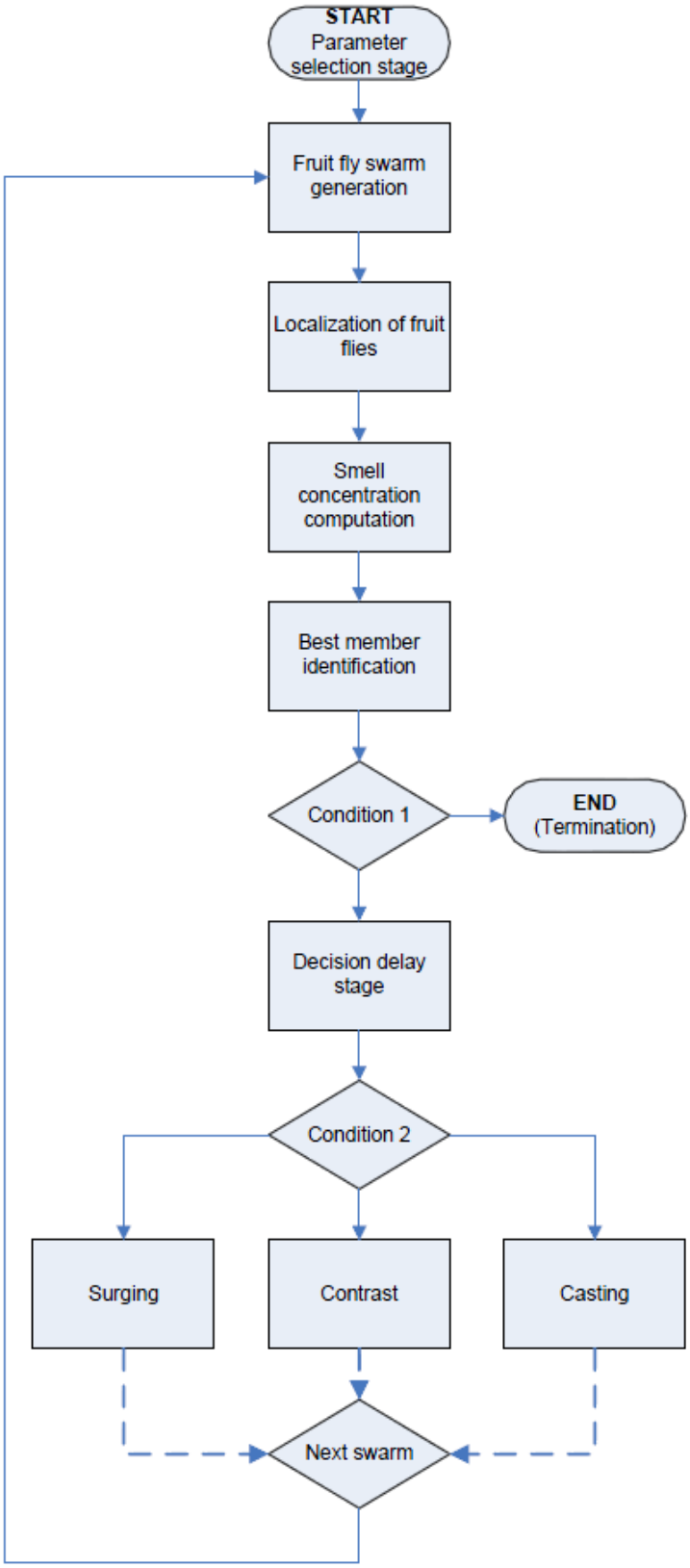

Fig. 1. Flowchart of the proposed c-mFOA algorithm.

3. Optimization results

Five machining processes essential to manufacturing industry were selected for optimizing their operational parameters using the proposed c-mFOA. The machining processes selected were turning; focused ion beam micro milling; laser cutting; wire electro-discharge machining and micro wire-electro discharge machining. In order to handle the aforementioned machining processes as multi-objective optimization problems, empirical models derived from designs of experiments and regression analyses presented in the literature, were considered as objective functions for the c-mFOA.

3.1 Turning

The empirical models of Palanikumar et al. (2009) were adopted to solve the optimization problem for the turning process of glass fiber reinforced plastic with PCD cutting insert. Rao et al. (2016) as well as Zou et al. (2014) were also took advantage of the same empirical models to present results from the corresponding turning optimization problem using NSTLBO and MOTLBO algorithms respectively. In the work of Palanikumar et al. (2009) the turning problem involved cutting speed *U (m/min)*, feed rate *f (mm/rev)* and depth of cut *a (mm)* as its process parameters whilst tool flank wear V_b *(mm),* surface roughness R_a *(μm)* and material removal rate *MRR* (mm^3/min) were the optimization objectives. The problem requires minimizing tool flank wear and surface roughness and maximizing material removal rate. The empirical models used as objective functions for the turning problem are given in Eq. 7, Eq. 8 and Eq. 9 for the three objectives respectively.

$$\text{Min}V_b = 0.09981+0.00069U+1.41111f-0.17944a+0.000001U^2-3.11111f^2+0.00222a^2-0.00267Uf+0.00007Ua+0.96667fa \quad (7)$$

$$\text{Min}R_a = 1.9065-0.0103U+11.1889f+0.3283a+0.000001U^2-7.1111\ f^2+0.0022a^2+0.0340Uf-0.0015Ua-4.433fa \quad (8)$$

$$\text{Max}MRR = 1000Uf\ a \quad (9)$$

where $50 \le U \le 150$; $0.1 \le f \le 0.20$ and $0.5 \le a \le 1.5$ are the process parameters' bounds for *U, f* and *a* respectively. The same problem is solved by employing the c-mFOA and two other modern meta-heuristics namely multi-objective grey wolf optimization algorithm-MOGWO (Mirjalili et al. 2016) and multi-objective multi-universe optimization algorithm-MOMVO (Mirjalili et al. 2017) so as to fairly compare the results. All algorithms were developed and deployed in *Mathworks MATLAB® R2013.*

Palanikumar et al. (2009) implemented the NSGA-II algorithm with a population size of 100 individuals and 100 generations (10.000 function evaluations). The same algorithm parameters where also adopted by Zou et al. (2014) as well as Rao et al. (2016) for rigorous comparisons. The problem is solved with the three aforementioned algorithms; c-mFOA; MOGWO and MOMVO to compare the results using the same number of population and generations. 60; 48 and 43 non-dominated solutions were obtained by c-mFOA; MOGWO and MOMVO algorithms respectively whilst best and worst results are summarized in Table 1.

Table 1. Best and worst set of the non-dominated solutions for turning process.

Algorithm	Results	Objectives		
		V_b (mm)	R_a (μm)	MRR (mm^3/min)
NSTLBO	Best	0.122	1.437	44989.703
	Worst	0.345	2.293	08138.912
c-mFOA	Best	0.119	1.512	41973.010
	Worst	0.339	2.348	07020.418
MOGWO	Best	0.138	1.523	40770.670
	Worst	0.321	2.146	10364.510
MOMVO	Best	0.134	1.554	41963.850
	Worst	0.328	2.367	06524.396

The non-dominated solutions obtained by c-mFOA as well as MOGWO and MOMVO are qualitatively compared with reference to those reported by Rao et al. (2016) using NSTLBO for the turning problem. Fig.1 illustrates the non-dominated solutions for all algorithms tested in the form of Pareto fronts. Fig.1a shows the Pareto front corresponding to the non-dominated solutions of NSTLBO; Fig.1b to the non-dominated solutions of the proposed c-mFOA; Fig.1c to the non-dominated solutions of MOGWO and Fig.1d to the non-dominated solutions of MOMVO.

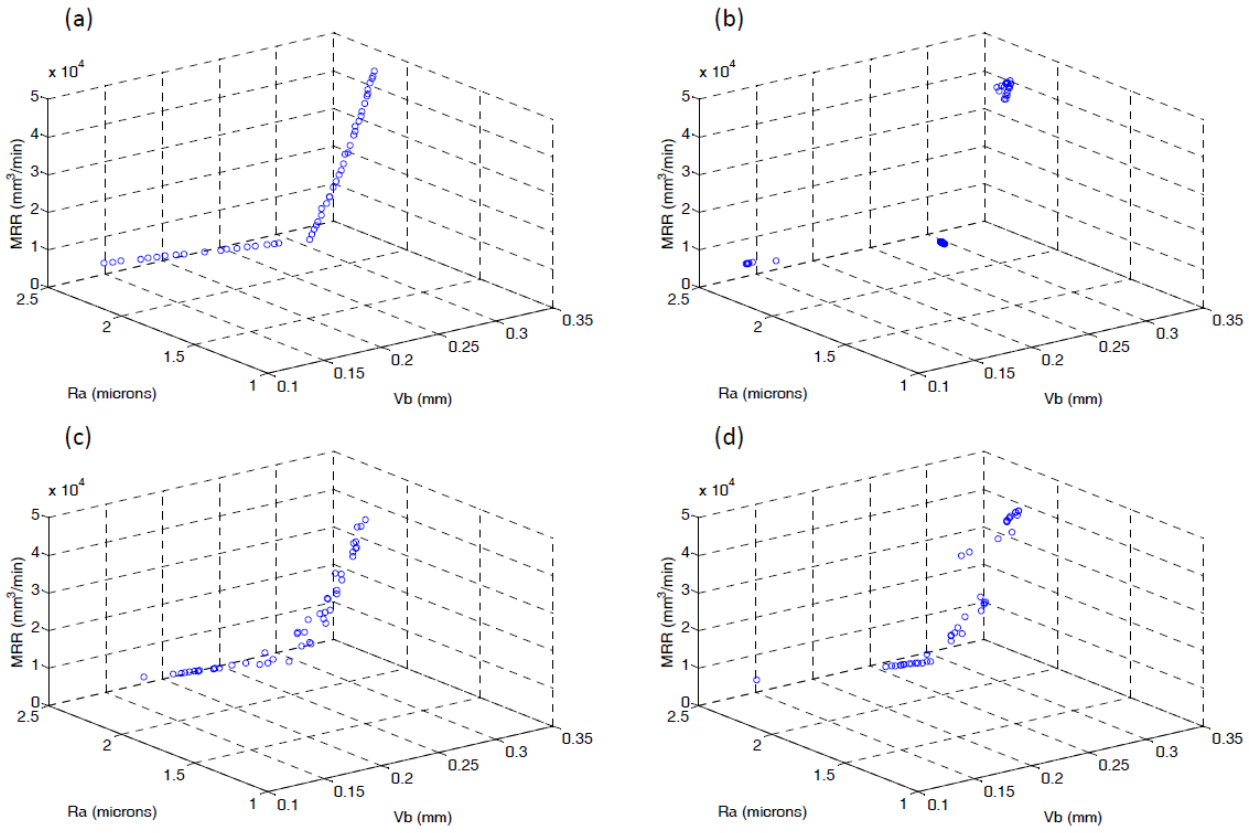

Fig. 1 Comparison of non-dominated solutions obtained for turning using: (a) NSTLBO (Rao et al. 2016), (b) c-mFOA; (c) MOGWO; (d) MOMVO.

It can be seen that compared to the non-dominated solutions of competitive algorithms, the ones obtained by c-mFOA are located to discrete regions of the Pareto front favoring all optimization criteria and no intermediate solutions are observed. Tool flank wear increases as cutting speed and feed rate increase whilst it reduces when increasing depth of cut. Thus, minimum values for cutting speed and feed rate are required to reduce tool flank wear along with a maximum value for depth of cut. To minimize tool flank wear V_b *(mm),* c-mFOA proposed low cutting speed U = 50.0284 *m/min*, (close to the lower bound of 50 *m/min*); low feed rate f = 0.1 *mm/rev*, which is the lower bound for feed rate and depth of cut a = 1.4999 *mm.* Surface roughness reduces by increasing cutting speed, yet; it increases by increasing feed rate. The interaction effect between feed rate and depth of cut is important to surface roughness whilst the effect of depth of cut alone is insignificant. Roughness reduces as the interaction between feed rate and depth of cut increases, thus high values for cutting speed; low values for feed rate and maximum values for depth of cut are required to minimize surface roughness. Accordingly, the c-mFOA has suggested cutting speed's value close to its upper level; the value of feed rate to its lower bound and the value of depth of cut to its lower bound as well (U = *141.4214 m/min*, rate f = 0.1 *mm/rev*, a = 1.5 *mm*). Material removal rate involves all three cutting conditions as a product when it comes to turning and milling and implies that high values for the cutting conditions are required for productivity. Therefore the c-mFOA has suggested values close to upper levels for all parameters; U = *141.4214 m/min*, rate f = 0.2 *mm/rev*, a = 1.4832 *mm.* The aforementioned results were found to be in consistency and good agreement with the experimental observations mentioned in Palanikumar et al. (2009).

Several quality and performance indicators for evaluating Pareto fronts have been proposed so far such as Hyper-volume, spacing, coverage, consolidation ratio, etc., yet no complete agreement on what metrics should be employed exists (Mirjalili and Lewis 2015). To provide a straightforward solution on assessing Pareto fronts as well as to emphasize to the practical merit when selecting a non-dominated solution among many while studying the difference between two algorithms under a more meaningful fashion, a statistical significance test was conducted. The two-sample t-test was selected to examine the populations of independent solutions for all objectives between NSTLBO and the proposed c-mFOA to judge profound superiority or to agree on similarity. Table 2 summarizes the results of the statistical significance test conducted between the solutions of NSTLBO -as the most competitive algorithm- and proposed c-mFOA.

Table 2. Two-sample t-test results for c-mFOA against NSTLBO for the turning problem.

Objective	Pair	Size N	Mean	StDev	T-value	P-value	Pooled StDev
V_b *(mm)*	NSTLBO	50	0.2297	0.0708	0.23	0.818	0.0741
	c-mFOA	60	0.2264	0.0768			
R_a *(μm)*	NSTLBO	50	1.853	0.241	0.22	0.823	0.3163
	c-mFOA	60	1.839	0.367			
MRR (mm^3/min)	NSTLBO	50	26762	11069	0.57	0.570	11144.4184
	c-mFOA	60	25547	11207			

With reference to the results obtained from the statistical significance test concerning the three optimization objectives of turning process It can be concluded that their small differences do not practically yield a significant difference referring to NSTLBO's and c-mFOA's non-dominated solutions. The selection of one among the multiple non-dominated solutions can be made according to individual

production demands and user's preferences concerning less tool flank wear; better surface finish and high production rates.

3.2 Focused ion beam micro-milling

The empirical models of Bhavsar et al. (2015) were adopted to solve the optimization problem for the focused ion beam (FIB) micro-milling of cemented carbide based on experimental data. In their work five process parameters were investigated namely extraction voltage x_1 *(kV)*; inclination angle x_2 *(deg)*; beam current x_3 *(nA)*; dwell time x_4 *(µs)* and pass overlap x_5 *(%)*. The optimization objectives under interest were *MRR* ($\mu m^3/sec$) for maximization and surface roughness R_a *(nm)* for minimization. The empirical models generated by Bhavsar et al. (2015) and used as objective functions for the FIB problem are given in Eq. 10 and Eq. 11 for the two objectives respectively.

$$MaxMRR = 0.0514-0.00506x_1-0.0269x_3-0.000032x_2^2-0.00009x_5^2-0.000103x_1x_2+0.0036x_1x_3+0.000228x_1x_5+0.000625x_2x_3+0.0001x_2x_5+0.000514x_3x_5 \quad (10)$$

$$MinR_a = 245+3.61x_2-5.38x_5-0.304x_1^2+0.0428x_2^2+0.0735x_5^2+0.863x_1x_3+0.144x_1x_5-0.17x_2x_3-0.139x_2x_5+1.5x_3x_4 \quad (11)$$

where $15 \le x_1 \le 30$; $10 \le x_2 \le 70$; $0.03 \le x_3 \le 3.5$; $1 \le x_4 \le 10$ and $30 \le x_5 \le 75$ are the process parameters' bounds for x_1, x_2, x_3, x_4 and x_5 respectively. Bhavsar et al. (2015) solved the problem using NSGA II algorithm with a population size equal to 60 and maximum number of generations equal to 1000 thus, having 60000 function evaluations. Rao et al. (2015) used NSTLBO to solve the same problem with the same parameter settings for fair comparisons. The problem is solved with the three algorithms; c-mFOA; MOGWO and MOMVO to compare the results using the same number of population and generations. 21; 50 and 46 non-dominated solutions were obtained by c-mFOA; MOGWO and MOMVO algorithms respectively whilst best and worst results are summarized in Table 3.

Table 3. Best and worst set of the non-dominated solutions for FIB micro-milling process.

Algorithm	Results	Objectives	
		R_a *(nm)*	*MRR* ($\mu m^3/sec$)
NSTLBO	Best	5.2024	0.6302
	Worst	92.2225	0.0228
c-mFOA	Best	4.824	0.6191
	Worst	102.787	0.0211
MOGWO	Best	8.1690	0.5437
	Worst	85.8215	0.0346
MOMVO	Best	60.067	0.6070
	Worst	90.404	0.2913

The non-dominated solutions obtained by c-mFOA as well as MOGWO and MOMVO are qualitatively compared with reference to those reported by Rao et al. (2016) using NSTLBO for the FIB

micro-milling problem. Fig.2 illustrates the non-dominated solutions for all algorithms tested in the form of Pareto fronts. Fig.2a shows the Pareto front corresponding to the non-dominated solutions of NSTLBO; Fig.2b to the non-dominated solutions of the proposed c-mFOA; Fig.2c to the non-dominated solutions of MOGWO and Fig.2d to the non-dominated solutions of MOMVO.

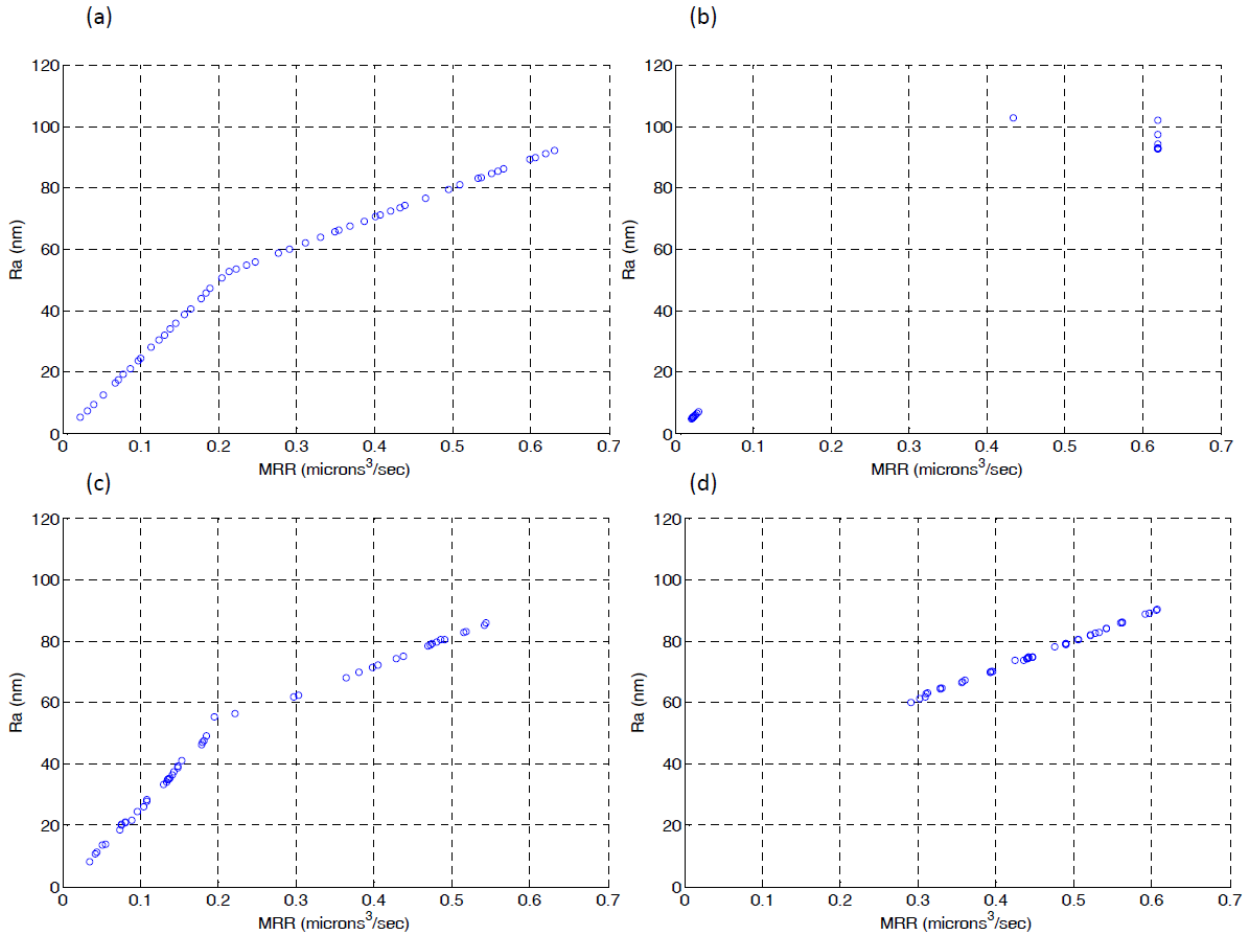

Fig. 2 Comparison of non-dominated solutions obtained for FIB micro-milling using: (a) NSTLBO (Rao et al. 2016), (b) c-mFOA; (c) MOGWO; (d) MOMVO.

It can be seen that compared to the non-dominated solutions of competitive algorithms, the ones obtained by c-mFOA are located to discrete regions of the Pareto front favoring the two optimization criteria whilst no intermediate solutions are observed. According to Bhavsar et al. (2015) NSGA-II suggested 13.97 *nm* and 0.5314 $\mu m^3/sec$ as the optimal results for surface roughness and material removal rate respectively. For the same problem NSTLBO suggested 5.2024 *nm* for surface roughness and 0.6302 $\mu m^3/sec$ for material removal rate. These results are 62.76% and 15.67% more advantageous for R_a and *MRR* respectively. The c-mFOA proposed in this work suggested optimal results equal to 4.824 *nm* and 0.6191 $\mu m^3/sec$ for R_a and *MRR* respectively. The result proposed by c-mFOA for R_a is 7.27% better than the one proposed by NSTLBO and 65.47% better than the one proposed by NSGA-II. The result proposed by c-mFOA for *MRR* is 14.17% better than the one proposed by NSGA-II whilst it is

slightly worst (1.76%) than the one proposed by NSTLBO. The values of extraction voltage, inclination angle and beam current should be as close as possible to their upper bounds for increasing MRR whereas dwell time is preferred to be at its lower bound. To achieve a maximum value of *MRR c-mFOA* has suggested values for extraction voltage, angle of incidence, beam current and overlap close to their upper bound whereas a value close to the lower bound was suggested for dwell time (i.e. x_1 =29.996 *kV*, x_2 = 69.99◦, x_3 = 3.499 *nA*, x_4 = 1.04 *μs* and x_5 =70.71*%*). *MRR* and *R*a are conflicting objectives, that is; as *MRR* increases *R*a increases as well. An increase in beam current tends to increase positive ions affecting the work material thus increasing the *MRR*. An increased value of inclination angle is also responsible to increase *MRR,* yet; it also increases R_a. Hence, to attain a reduced value of R_a, lower values for beam current and inclination angle are preferable. In addition, a reduced value for dwell time results in reduced *R*a, whilst extraction voltage has insignificant impact on R_a. The c-mFOA has selected the values for FIB micro-milling parameters to minimize R_a accordingly (i.e. x_1 =29.99 *kV*, x_2 = 10◦, x_3 = 0.014 *nA*, x_4 = 2.53 *μs* and x_5 = 30 %). The non-dominated set of solutions provided by c-mFOA for the FIB micro-milling problem facilitates users on selecting a solution which may satisfy their demands of either high *MRR* or low *R*a so as to meet production specifications.

3.3 Laser cutting

The empirical models of Padney and Dubey (2012) were adopted to solve the optimization problem for the laser cutting process based on experimental data. In their work four process parameters were investigated namely gas pressure x_1 *(kg/cm²)*; pulse width x_2 *(ms)*; pulse frequency x_3 *(Hz)* and cutting speed x_4 *(mm/min).* The optimization objectives under interest were surface roughness R_a *(μm)* and kerf taper k_t *(deg)*; both for minimization. The empirical models generated by Padney and Dubey (2012) and used as objective functions for the laser cutting problem are given in Eq. 12 and Eq. 13 for the two objectives respectively.

$$Min R_a = -33.4550+7.2650x_1+12.1910x_2+1.8114x_3-0.2813x_1^2-0.0726x_3^2-0.0055x_4^2-1.7719x_1x_2 \quad (12)$$

$$Min k_t = 8.5670-2.5280x_1+0.2093x_1^2+2.1318x_2^2-0.0371x_3^2-0.7193x_1x_2+0.0108x_3x_4+0.0752x_1x_3 \quad (13)$$

where $5 \le x_1 \le 9$; $1.4 \le x_2 \le 2.2$; $6 \le x_3 \le 14$; and $15 \le x_4 \le 25$ are the process parameters' bounds for x_1, x_2, x_3 and x_4 respectively. Padney and Dubey (2012) solved the problem using a genetic algorithm (GA) with a population size equal to 200 and maximum number of generations equal to 800 thus, having 160000 function evaluations. Rao et al. (2015) used NSTLBO to solve the same problem with the same parameter settings for fair comparisons. The problem is solved with the three algorithms; c-mFOA; MOGWO and MOMVO to compare the results using the same number of population and generations. 21; 50 and 27 non-dominated solutions were obtained by c-mFOA; MOGWO and MOMVO algorithms respectively whilst best and worst results are summarized in Table 4. The non-dominated solutions obtained by c-mFOA as well as MOGWO and MOMVO are qualitatively compared with reference to those reported by Rao et al. (2016) using NSTLBO for the laser cutting problem. Fig. 3 illustrates the non-dominated solutions for all algorithms tested in the form of Pareto fronts. Fig. 3a shows the Pareto front corresponding to the non-dominated solutions of NSTLBO; Fig. 3b to the non-dominated solutions of the

proposed c-mFOA; Fig. 3c to the non-dominated solutions of MOGWO and Fig. 3d to the non-dominated solutions of MOMVO.

Table 4. Best and worst set of the non-dominated solutions for laser cutting process.

Algorithm	Results	Objectives	
		R_a (μm)	K_t (deg)
NSTLBO	Best	5.3189	0.3822
	Worst	11.9862	2.8431
c-mFOA	Best	5.3262	0.3839
	Worst	11.9876	2.8471
MOGWO	Best	5.3873	0.4969
	Worst	10.7574	2.8269
MOMVO	Best	5.6604	1.0570
	Worst	10.4770	3.1087

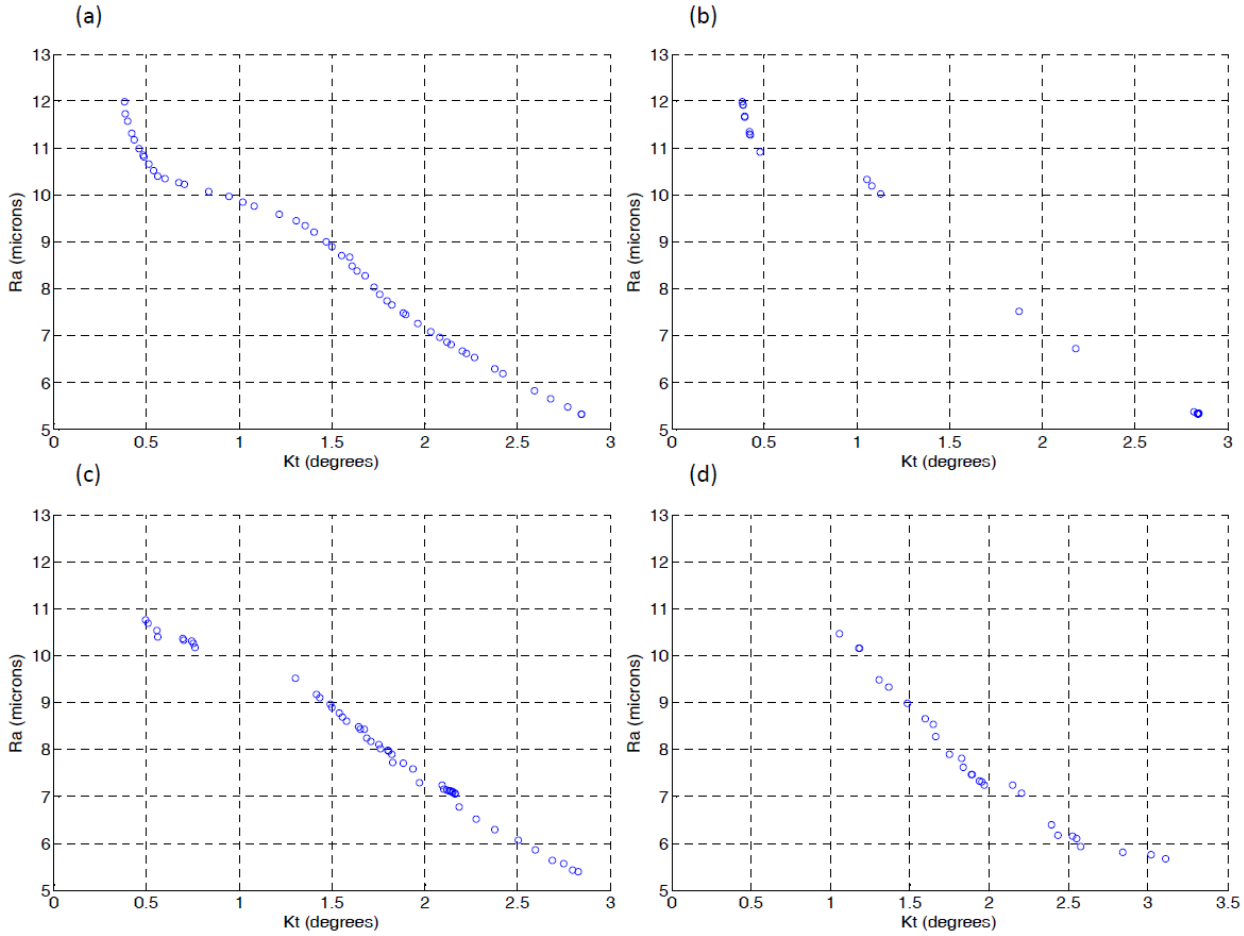

Fig. 3 Comparison of non-dominated solutions obtained for laser cutting using: (a) NSTLBO (Rao et al. 2016), (b) c-mFOA; (c) MOGWO; (d) MOMVO.

It is observed from Fig. 3 that the Pareto fronts obtained by NSTLBO and c-mFOA are of the same quality with the noticeable difference on c-mFOA to provide less intermediate solutions that those provided by NSTLBO. However the sets of independent non-dominated solutions obtained by both algorithms lie practically in the same region of their corresponding Pareto fronts. The solutions of c-mFOA agree with the original experimental observations of Padney and Dubey (2012). Kerf taper k_t reduces with the increase of gas pressure at low values for pulse width. Nevertheless, at high values of pulse width, k_t reduces and then gradually increases by increasing gas pressure. K_t increases with the increase in gas pressure whilst pulse width is maintained at its lower bound. Kerf taper k_t also increases at higher values of pulse width by increasing gas pressure. Consequently, since pulse width is not advantageous for k_t it is maintained at its lower bound for all non-dominated solutions. Surface roughness R_a increases under high cutting speed for both high and low values of pulse frequency. Accordingly, R_a increases as cutting speed increases from lower to upper level whereas pulse frequency is maintained for both high and low levels. The c-mFOA obtained the optimal solution of R_a = 5.3262 μm for x_1=5.0013 kg/cm^2; x_2=1.4003 ms, x_3=6.0009 Hz and x_4=24.9901 mm/min and obtained the optimal solution of k_t = 0.3839 deg, for x_1=5.9318 kg/cm^2; x_2=1.4006 ms, x_3=13.9994 Hz and x_4=15.0024 mm/min. By comparing the optimal values for k_t and R_a obtained by NSTLBO and c-mFOA (Table 4) it can be seen that the differences are insignificant. This has been also justified by conducting a statistical significance test (two sample t-test) using the independent sets of non-dominated solutions provided by NSTLBO and c-mFOA algorithms. Table 5 summarizes the results from the significance test whilst it can be observed that p-values are by far larger than 0.05.

Table 5. Two-sample t-test results for c-mFOA against NSTLBO for the laser cutting problem.

Objective	Pair	Size N	Mean	StDev	T-value	P-value	Pooled StDev
R_a (μm)	NSTLBO	50	8.63	1.91	-0.40	0.690	2.2303
	c-mFOA	21	8.86	2.87			
K_t (deg)	NSTLBO	50	1.474	0.765	0.02	0.987	0.8765
	c-mFOA	21	1.470	1.10			

3.4 Wire electro-discharge machining

The empirical models of Garg et al. (2012) were adopted to solve the optimization problem for wire electro-discharge machining (wEDM) based on experimental data. In their work six process parameters were investigated namely pulse-on time T_{on} (μs); pulse-off time T_{off} (μs); peak current IP (A); spark set voltage SV (V); wire feed WF (m/min) and wire tension WT (g). The optimization objectives under interest involved maximization of cutting speed U (mm/min) and minimization of surface roughness R_a (μm). The empirical models generated by Garg et al. (2012) and used as objective functions for the wEDM problem are given in Eq. 14 and Eq. 15 for the two objectives respectively.

$$maxU = -24.85563 + 0.29637\times T_{on} + 0.12237\times T_{off} + (6.53472E-4)\times IP + 0.1454\times SV + 0.060880\times WT + (1.52323E-3)\times T_{off}^2 - (3.15625E-3)\times T_{on}\times T_{off} - (1.66667E-3)\times T_{on}\times SV + (7.84375E-4)\times T_{off}\times SV - (1.30312E-3)\times SV\times WT \quad (14)$$

$$MinR_a = 2.28046 + (0.014514 \times T_{on}) - 0.01175 \times T_{off} - (7.54444E-3) \times IP - (4.466E-3) \times SV - 0.19140 \times WF - 0.8279 \times WT + (7.35417E-3) \times T_{on} \times WT + (1.08333E-3) \times IP \times WF \quad (15)$$

where $112 \leq T_{on} \leq 118$; $48 \leq T_{off} \leq 56$; $140 \leq IP \leq 200$; $35 \leq SV \leq 55$; $6 \leq WF \leq 10$ and $4 \leq WT \leq 8$ are the process parameters' bounds for T_{on}, T_{off}, *IP, SV, WF* and *WT* respectively. Garg et al. (2012) solved the problem using the NSGA-II with a population size equal to 100 and maximum number of generations equal to 1000 thus, having 100000 function evaluations. Rao et al. (2015) used NSTLBO to solve the same problem with the same parameter settings for fair comparisons. The problem is solved with the three algorithms; c-mFOA; MOGWO and MOMVO to compare the results using the same number of population and generations. 21; 39 and 47 non-dominated solutions were obtained by c-mFOA; MOGWO and MOMVO algorithms respectively whilst best and worst results are summarized in Table 6. The non-dominated solutions obtained by c-mFOA as well as MOGWO and MOMVO are qualitatively compared with reference to those reported by Rao et al. (2016) using NSTLBO for the wEDM problem. Fig. 4 illustrates the non-dominated solutions for all algorithms tested in the form of Pareto fronts. Fig. 4a shows the Pareto front corresponding to the non-dominated solutions of NSTLBO; Fig. 4b to the non-dominated solutions of the proposed c-mFOA; Fig. 4c to the non-dominated solutions of MOGWO and Fig. 4d to the non-dominated solutions of MOMVO.

Table 6. Best and worst set of the non-dominated solutions for wEDM.

Algorithm	Results	Objectives	
		U (mm/min)	R_a *(μm)*
NSTLBO	Best	1.3971	1.5150
	Worst	0.3227	2.2307
c-mFOA	Best	1.6604	1.9286
	Worst	0.6922	2.2972
MOGWO	Best	1.5699	1.9361
	Worst	0.7560	2.2739
MOMVO	Best	0.5608	1.9397
	Worst	0.2010	2.1652

It can be observed form Fig. 4 that the non-dominated solutions provided by c-mFOA, MOGWO and MOMVO do not exhibit the same distribution as the one shown for NSTLBO. Nevertheless the values for process parameters were checked for their validity and found consistent despite their different topology in the corresponding Pareto fronts. In order to substantiate the solutions obtained by c-mFOA the pairs of process parameters that resulted to best objective values for cutting speed and surface roughness were examined. Cutting speed was maximized for T_{on} = 117.9832 *μs*; T_{off} = 148.0143 *μs; IP* = 140.6924 *A; SV* = 35.0202 *V; WF* = 9.9962 *m/min* and *WT* = 4.0092 *g.* Indeed cutting speed increases with the increase of pulse-on time and peak current, yet; it reduces with the increase of pulse-off time and spark gap voltage. Wire tension is insignificant to cutting speed. Thus to maintain high cutting speed, c-mFOA has selected a value close to upper bound for pulse-on time and values close to the lower bounds for pulse-off time and spark gap voltage. Accordingly, to maintain minimum surface roughness, c-mFOA algorithm has selected lower bound values for pulse-on time (T_{on} = 112.0114 *μs*) and peak current (*IP* = 140.0760 *A*) whilst it selected upper bound values for pulse-off time (T_{off} = 55.9903 *μs*) and wire feed

(*WF* = 9.9577 *m/min*). In this case the c-mFOA was found to be inferior compared to the NSTLBO algorithm at least for the same number of function evaluations.

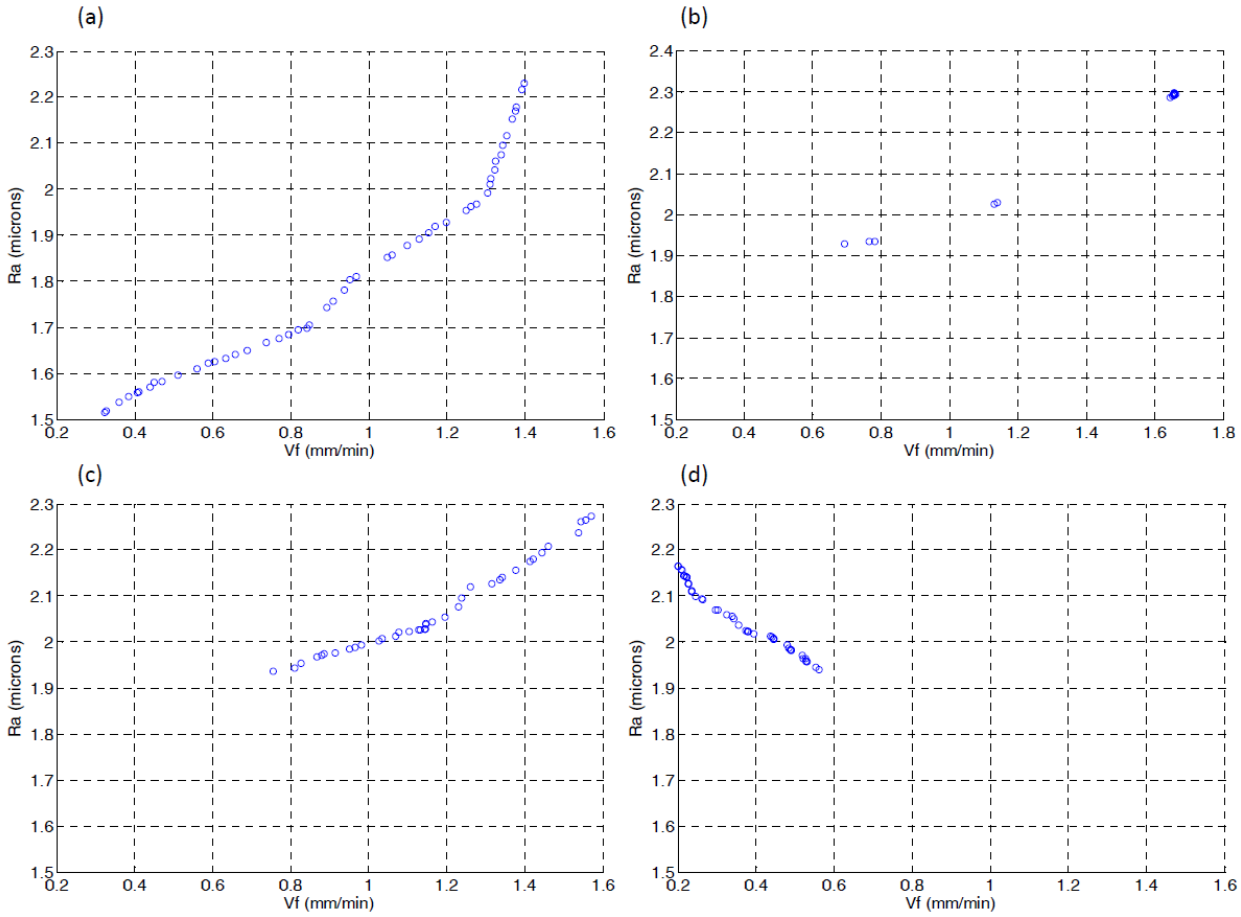

Fig. 4 Comparison of non-dominated solutions obtained for wEDM using: (a) NSTLBO (Rao et al. 2016), (b) c-mFOA; (c) MOGWO; (d) MOMVO.

3.5 Micro wire electro-discharge machining

The empirical models of Kuriachen et al. (2015) were adopted to solve the optimization problem for micro-wire electro-discharge machining (mwEDM) based on experimental data. In their work four process parameters were investigated namely gap voltage *GV (V)*; capacitance *C (µF)*; feed speed V_f *(µm/sec)* and wire tension *WT (gm).* The optimization objectives under interest involved maximization of material removal rate (mm^3/min) and minimization of surface roughness R_a *(µm)*. The empirical models generated by Kuriachen et al. (2015) and used as objective functions for the mwEDM problem are given in Eq. 16 and Eq. 17 for the two objectives respectively.

$$max\sqrt{MRR} = 0.14+0.006812xGV+0.024xC+0.014xV_f-0.007979xGVxC+0.0385xCxV_f-0.039C^2 \quad (16)$$

$$Min R_a = 1.13 - 0.11 x GV + 0.080 x C - 0.17 x V_f - 0.16 x C x V_f + 0.60 x GV^2 + 0.28 x V_f^2 \quad (17)$$

where $100 \leq GV \leq 150$; $0.01 \leq C \leq 0.4$; $3 \leq V_f \leq 9$ and $5\%\ (4.125) \leq Wt \leq 15\%\ (12.375)$ are the process parameters' bounds for *GV, C,* V_f, and *WT* respectively. Kuriachen et al. (2015) solved the problem using the PSO algorithm by using a combined objective function via fuzzy logic. Unfortunately their approach provided a single solution suggesting maximum *MRR* equal to $0.0230\ mm^3/min$ and minimum R_a equal to $1.3386\ \mu m$ for *GV* = 113 *V*; *C*=0.26 μF and $V_f = 9\ \mu m/sec$. Rao et al. (2015) used NSTLBO to solve the same problem with the same parameter settings (i.e. population size 50 and maximum generation 20, thus; 2000 function evaluations) for fair comparisons. The problem is solved with the three algorithms; c-mFOA; MOGWO and MOMVO to compare the results using the same number of population and generations. 21; 50 and 49 non-dominated solutions were obtained by c-mFOA; MOGWO and MOMVO algorithms respectively whilst best and worst results are summarized in Table 7. The non-dominated solutions obtained by c-mFOA as well as MOGWO and MOMVO are qualitatively compared with reference to those reported by Rao et al. (2016) using NSTLBO for the mwEDM problem. Fig. 5 illustrates the non-dominated solutions for all algorithms tested in the form of Pareto fronts. Fig. 5a shows the Pareto front corresponding to the non-dominated solutions of NSTLBO; Fig. 5b to the non-dominated solutions of the proposed c-mFOA; Fig. 5c to the non-dominated solutions of MOGWO and Fig. 5d to the non-dominated solutions of MOMVO.

Table 7. Best and worst set of the non-dominated solutions for mwEDM.

Algorithm	Results	Objectives	
		MRR (mm^3/min)	R_a (μm)
NSTLBO	Best	0.0261	1.0799
	Worst	0.0157	1.3484
c-mFOA	Best	0.0321	0.8464
	Worst	0.0032	2.5645
MOGWO	Best	0.0273	1.8155
	Worst	0.0156	2.3809
MOMVO	Best	0.0308	1.1113
	Worst	0.0075	2.5050

With reference to best results obtained by NSTLBO and c-mFOA in terms of the optimization objectives *MRR* and R_a (Table 7) it can be deduced that c-mFOA is superior to PSO and NSTLBO in finding best values. For material removal rate the c-mFOA is 39.56% more beneficial than PSO and 18.69% more beneficial than NSTLBO according to its corresponding values. For surface roughness, c-mFOA algorithm is 36.78% more beneficial than PSO and 27.60% more beneficial than NSTLBO according to its corresponding values. According to the Pareto fronts depicted in Fig. 5, c-mFOA algorithm emphasized to regions where optimization objectives are facilitated whilst no intermediate solutions were provided. NSTLO algorithm provided a significant number of intermediate solutions, yet; it didn't manage to each global optima for *MRR* and R_a. The c-mFOA algorithm maximized MRR for *GV* = 141.4214 *V*; *C*=0.01 μF and $V_f = 9.0\ \mu m/sec$. The same optimum result of *MRR* may also be reached for capacitance *C* equal to 0.0384 µF which is an intermediate level value. Surface roughness was minimized by c-mFOA algorithm

for GV = 100.0022 V; C=0.2466 μF and V_f = 3.3036 $\mu m/sec$. These results are in agreement with the experimental observations of Kuriachen et al. (2015) for the mwEDM problem.

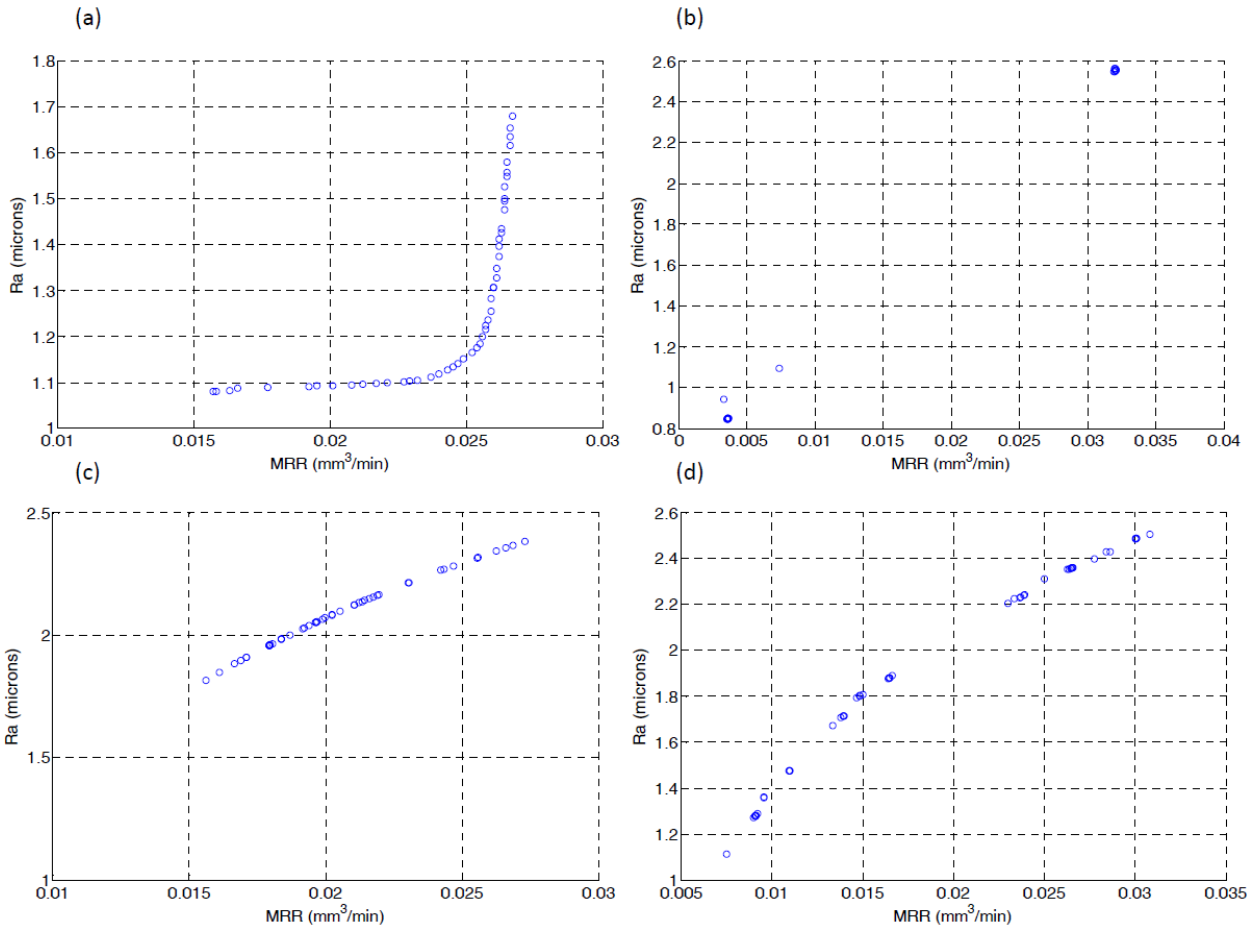

Fig. 5 Comparison of non-dominated solutions obtained for mwEDM using: (a) NSTLBO (Rao et al. 2016), (b) c-mFOA; (c) MOGWO; (d) MOMVO.

In order to facilitate the comparison among non-dominated solutions for the two-objective machining problems, FIB; Laser cutting; wEDM and mwEDM, additional comparative diagrams were prepared and illustrated in Fig. 6.

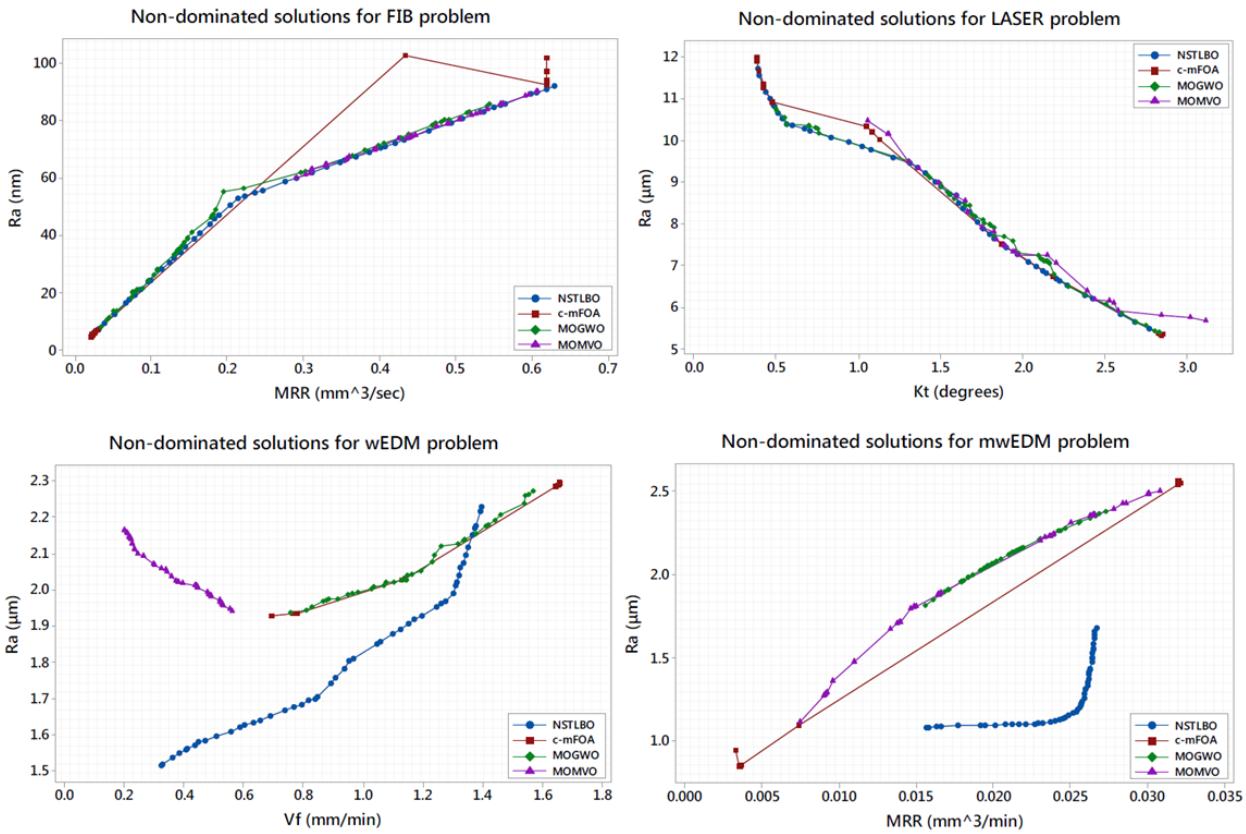

Fig. 6 Comparative diagrams of non-dominated solutions obtained by the algorithms for the machining problems examined.

4. Conclusions

The visual contrast-based fruit fly algorithm (c-mFOA) was implemented to solve five machining processes namely turning, focused ion-beam micro-milling; wire electro-discharge machining and micro-wire electro-discharge machining based on the mathematical models developed from experimental data by previous researchers. Two other algorithms namely multi-objective grey wolf optimizer (MOGWO) and multi-objective multi universe optimizer (MOMVO) were also tested. Comparison of results was made against the NSTLBO algorithm with emphasis to those obtained by the proposed c-mFOA. It was shown that c-mFOA can obtain consistent and reliable results not only for the machining operations presented in this work but a number of others as well. Comparisons were made using a statistical significance test where the solutions of NSTLBO and c-mFOA algorithms for the problems' optimization objectives were treated as independent populations. It was observed that, in most cases small differences among the results of NSTLBO and c-mFOA were not statistically significant from a practical perspective which means that c-mFOA is just as a robust and competitive algorithm as NSTLBO. By studying the Pareto fronts corresponding to the non-dominated solutions for the aforementioned problems it was found that c-mFOA focuses mainly in the areas of interest in terms of favouring the optimization objectives without the proposition of intermediate solutions, which is not necessarily a

drawback. However if the algorithm-specific parameters (i.e. surging, visual contrast and casting) are to be differently adjusted, the results referring to the non-dominated solutions can favour the selection of process parameters for different percentages of impact for the optimization objectives at hand.

According to the No-Free Lunch theorem (Wolpert and Macready, 1997) heuristics do not necessarily achieve best results to all kinds of engineering optimization problems. This fact leaves room for researchers to suggest new algorithms or improve current variants based on this aspect that there is no optimization algorithm capable of solving all optimization problems. From the results presented in this work concerning the optimization of conventional and non-conventional machining processes it is quite clear that the selected heuristics including the proposed c-mFOA yield variations in terms of their success in optimization. With reference to the fact that their objective functions formulate different solution domains and are products of regression models it is expected that their representations constitute complex search fields that in turn produce different Pareto fronts with either concave or convex properties and of different degree. Therefore it can be supported that the problem at hand is indeed responsible for the performance of a heuristic depending on its representation and corresponding solution domain. A straightforward way to study the behavior of a determined heuristic to an optimization problem is to conduct several parametric experiments with reference to a range of alternative settings referring to algorithm-specific parameters. It is believed by the authors that such a research as a future perspective will lead to the thorough understanding of the problems which the c-mFOA is likely to exhibit an even better operational state and finally determine the kind of problems that are well-suited for the proposed c-mFOA.

References (to be formatted according to the selected journal)

Acosta, M., Kanarachos, S. and Fitzpatrick, M. E., (2017). Optimized tire force estimation using extended Kalman filter and fruit fly optimization, *IECON 2017 - 43rd Annual Conference of the IEEE Industrial Electronics Society*, Beijing, 2017, pp. 4074-4079, doi: 10.1109/IECON.2017.8216698.

Palanikumar, K., Latha, B., Senthilkumar, V. S., & Karthikeyan, R. (2009). Multiple performance optimization inmachining of GFRP composites by a PCD tool using non-dominated sorting genetic algorithm (NSGA-II). *Metals and Materials International*, *15*(2), 249–258.

Srinivas, N., Deb, K. (1995). Multiobjective function optimization using non-dominated sorting genetic algorithms, *Evol. Comput.*, 2(3), 221-248.

Bhavsar, S.N., Aravindan, S., & Rao, P.V. (2012). Machinability Study of Cemented Carbide Using Focused Ion Beam (FIB) milling. Materials and Manufacturing Processes, 27(10), 1029–1034.

Bhavsar, S.N., Aravindan, S., & Rao, P.V. (2015). Investigating material removal rate and surface roughness using multi-objective optimization for focused ion beam (FIB) micro-milling of cemented carbide. *Precision Engineering*, *40*, 131–138.

Garg, M. P., Jain, A., & Bhushan, G. (2012). Modelling and multi-objective optimization of process parameters of wire electrical-discharge machining using non-dominated sorting genetic algorithm-II. *Proceedings of Institution of Mechanical Engineers: Part B-Journal of Engineering Manufacture*, *226*(12), 1986–2001.

Kuriachen, B., Somashekhar, K. P., & Mathew, J. (2015). Multi response optimization of micro-wire electrical discharge machining process. *International Journal of Advanced Manufacturing Technology*, *76*, 91–104.

Pandey, A. K., & Dubey, A. K. (2012). Simultaneous optimization of multiple quality characteristics in laser cutting of titanium alloy sheet. *Optics and Laser Technology*, *44*, 1858–1865.

Zou, F.,Wang, L.,Hei,X., Chen,D.,&Wang, B. (2014). Multi-objective optimization using teaching–learning-based optimization algorithm. *Engineering Applications of Artificial Intelligence*, *26*, 1291–1300.

Rao, R.V., Rai, D.P., Balic, J. (2016) Multi-objective optimization of machining and micro-machining processes using non-dominated sorting teaching–learning-based optimization algorithm, J Intell Manuf. DOI 10.1007/s10845-016-1210-5

Pan W (2012). A new fruit fly optimization algorithm: taking the financial distress model as an example. Knowl-Based Systems, 26(6) .

Li, J., Pan, Q., Mao, K., Suganthan, P. (2014). Solving the steelmaking casting problem using an effective fruit fly optimisation algorithm. Knowledge-Based Systems,72,28-36.

Pan W. Using modified fruit fly optimisation algorithm to perform the function test and case studies. Connect Sci 2013;25:151–60.

Pan Q, Sang H, Duan J, Gao L. An improved fruit fly optimization algorithm for continuous function optimization problems. Knowl-Based Syst 2014;62:69–83.

Wu L, Zuo C, Zhang H. (2015). A cloud model based fruit fly optimization algorithm. Knowledge-Based Systems, 89, 603-617.

Mitic, M., Vukovic, N., Petrovic, M., Miljkovic. Z. (2015). Chaotic fruit fly optimization algorithm. Knowledge-Based Systems, 89, 446-458.

Yuan X, Dai X, Zhao J, He Q (2014). On a novel multi-swarm fruit fly optimization algorithm and its application. Appl Math Comput 233, 260–71.

Kanarachos, S., Griffin, J., Fitzpatrick, M.E. (2017) Efficient truss optimization using the contrast-based fruit fly optimization algorithm, Computers and Structures, 182, 137-148.

Kanarachos, S., Savitski, D., Lagaros, N. and Fitzpatrick, M., 2017. Automotive magnetorheological dampers: modelling and parameter identification using contrast-based fruit fly optimisation. Soft Computing, 22(24), pp.8131-8149.

Mirjalili, S., Lewis, A. (2015). Novel performance metrics for robust multi-objective optimization algorithms, Swarm and Evolutionary Computation 21, 1-23.

Mirjalili, S., Saremi, S., Mirjalili, S.M., Coelho L. (2016). Multi-objective grey wolf optimizer: A novel algorithm for multi-criterion optimization. Expert Systems with Applications, 47, 106-119.

Mirjalili, S., Jangir, P., Mirjalili, S.Z., Saremi, S., Trivedi, I.N. (2017). Optimization of problems with multiple objectives using the multi-verse optimization algorithm, Knowledge-based Systems, DOI: http://dx.doi.org/10.1016/j.knosys.2017.07.018

Wolpert DH, Macready WG (1997) No free lunch theorems for optimization. IEEE Trans Evol Comput 1:67-82.